Author(s): Laitinen, Mikko; Sajavaara, Timo; Rossi, Mikko; Julin, Jaakko; Puurunen, R.L.; Suni, T.; Ishida, T.; Fujita, H.; Arstila, K.; Brijs, B.; Whitlow, Harry

Title: Depth profiling of Al2O3+ TiO2 nanolaminates by means of a time-of-flight energy spectromete

Year: 2011

Version:

MANUSCRIPT COVER PAGE

Beam Interactions with Materials and Atoms
Nuclear Instruments and Methods in Physics Research, Section B.

Paper Reference Number : O6
Title of Paper :

Depth profiling of $Al_2O_3+TiO_2$ nanolaminates by means of a time-of-flight energy spectrometer

Corresponding Author : Mikko Laitinen

Full Mailing Address : Dept. of Physics, P.O.Box 35, 40014 University of Jyväskylä, Finland

Telephone : +358 400994836
Fax : : +358 142602351
E-mail : mikko.i.laitinen@jyu.fi

Co-Author, email : timo.sajavaara@jyu.fi
Co-Author, email : mikko.rossi@jyu.fi
Co-Author, email : jaakko.julin@jyu.fi
Co-Author, email : riikka.puurunen@vtt.fi
Co-Author, email : tommi.suni@vtt.fi
Co-Author, email : tadashii@iis.u-tokyo.ac.jp
Co-Author, email : fujita@iis.u-tokyo.ac.jp
Co-Author, email : kai.arstila@imec.be
Co-Author, email : bert.brijs@imec.be
Co-Author, email : harry.j.whitlow@jyu.fi

Keywords: ToF-ERDA, ERD, depth profiling, Al_2O_3 TiO_2, nanolaminate, ALD

Number of characters (using "character count")   = A = 14900

Number of 1-column tables or figures   = B = 3

Number of 2-column tables or figures   = C = 2

   Estimated number of printed pages   = (A + 1300B + 5000C)/8500   = 3.39

Depth profiling of Al₂O₃+TiO₂ nanolaminates by means of a time-of-flight energy spectrometer

M. Laitinen[1], T. Sajavaara[1], M. Rossi[1], J. Julin[1], R.L. Puurunen[2], T. Suni[2,3],

T. Ishida[3], H. Fujita[3], K. Arstila[4], B. Brijs[4], H.J. Whitlow[1]

[1]*Dept. of Physics, P.O.Box 35, 40014 University of Jyväskylä, Finland, mikko.i.laitinen@jyu.fi*

[2]*VTT Technical Research Centre of Finland, Tietotie 3, FI-02150 Espoo, Finland*

[3]*Institute of Industrial Science, University of Tokyo*

ew304, 4-6-1 Komaba, Meguro-ku, 153-8505 Tokyo, Japan

[4]*Imec, Kapeldreef 75, Leuven 3001, Belgium*

Abstract:

Atomic layer deposition (ALD) is currently a widespread method to grow conformal thin films with a sub-nm thickness control. By using ALD for nanolaminate oxides, it is possible to fine tune the electrical, optical and mechanical properties of thin films. In this study the elemental depth profiles and surface roughnesses were determined for Al₂O₃+TiO₂ nanolaminates with nominal single-layer thicknesses of 1, 2, 5, 10 and 20 nm and total thickness between 40 nm and 60 nm. The depth profiles were measured by means of a time-of-flight elastic recoil detection analysis (ToF-ERDA) spectrometer recently installed at the University of Jyväskylä. In TOF-E measurements ^{63}Cu, ^{35}Cl, ^{12}C and ^{4}He ions with energies ranging from 0.5 to 10 MeV, were used and depth profiles of the whole nanolaminate film could be analyzed down to 5 nm individual layer thickness.

Introduction

Use of atomic layer deposition (ALD) [1] in the thin film applications related to microelectronics industry is widely recognized. There is, however, a wide range of other applications for the ALD films as well. These include the original use of ALD invention for making electroluminescent displays [2], growth of bone-like mineral hydroxyapatite [3] for biocompatible surfaces [4] and dye-sensitized solar cell applications where ALD coatings enhance the conversion efficiency of the sunlight [5]. Also the silicon dioxide insulating layer in the silicon-on-insulator (SOI) wafers can nowadays be replaced by atomic layer deposited oxides [6]. Recently, the use of ALD-Al_2O_3 and -TiO_2 films in MEMS applications has also been studied [7]. By using ALD nanolaminates, it is possible to both fine tune the roughness of the surface layer [8] [9] and select a proper layer composition for different electrical [10], optical [11] or hard coating [12] applications.

Elemental depth profiling of the nanolaminate films is challenging for a number of reasons. An ideal technique would provide quantitative information on the elemental composition and thickness of individual layers from the surface to the substrate interface. The composition analysis should also include low-level light impurities like H and C. These requirements are hard to reach by any analysis technique, especially in the case of Al_2O_3+TiO_2 nanolaminate film, which is insulating and consists of fairly light elements. An extra difficulty for scattering techniques is the five natural isotopes of Ti, which makes the data analysis more challenging. In other studies Auger electron spectroscopy [13] and scanning electron microscope equipped with energy dispersive X-ray detector [14] have earlier been used for depth profiling mainly Al and Ti in Al_2O_3+TiO_2 nanolaminates.

In this work we have used MeV ions to analyze the samples in conjunction with a time-of-flight-energy spectrometer [15] [16] in a forward scattering direction for the detection of scattered incident ions and recoiled sample atoms. In the analysis both scattered incident ions and sample recoils were used in order to maximize the information from the sample.

Experimental

Al_2O_3+TiO_2 nanolaminate films were atomic layer deposited on 150 mm Si wafers using Picosun SUNALE[TM] R-150 ALD reactor and $Al(CH_3)_3$/H_2O and $TiCl_4$/H_2O processes for Al_2O_3 and TiO_2 films, respectively. The surface roughnesses of the films were measured with a NanoScope IV atomic force microscope (AFM) in a tapping mode. Similar samples (8×(2 nm Al_2O_3 +3 nm TiO_2)) were also measured with Hitachi HD-2300 transmission electron microscope (TEM) equipped with an energy dispersive X-ray (EDX) detector. The TEM cross sectional sample was prepared with Hitachi FB2100 focused ion beam (FIB) and the sample thickness was ~200 nm after thinning. 200 kV acceleration voltage was used for the observation. Five different sample sets were prepared with total film thicknesses between 41 nm and 60 nm (see Table 1).

Depth profiles of the samples were measured with a newly built time-of-flight elastic recoil detection analysis (ToF-ERDA) spectrometer, which is installed in one of the beam lines of the 1.7 MV Pelletron accelerator at the Accelerator Laboratory of the University of Jyväskylä. The time-of-flight–energy spectrometer consists of two carbon-foil time pickoff detectors 633 mm apart followed by a Si charged particle detector as an energy detector. In the timing gates, when recoiled ions traverse thin carbon foils (having thickness of 3 and 10 $\mu g/cm^2$, for the first and the second detector, respectively), secondary electrons are emitted and these electrons are guided to an MCP detector, where they are multiplied [17]. The time-of-flight and therefore velocity of the

3

ion is determined from the time difference of the anode signals of the two timing detectors. Signals from timing gate and energy detector are amplified and digital data is collected from ADC/TDC unit in a time-stamped mode by National Instruments FPGA card and LabVIEW program. Time-stamping data allows ToF-E–coincidence events to be determined offline with a resolution of 25 ns. The timing resolution of the spectrometer was measured to be 155 ps for 4.8 MeV ^{4}He^{2+} ions scattered from a thin (1-2 nm) Au film on a Si substrate. The energy dependent detection efficiency of the ToF detector for H and He was measured to be 35–65% and 92%, respectively, for the energy range used in this study. Detection efficiency for carbon was measured to be >99.5%.

In the measurements ^{35}Cl^{5+}, ^{63}Cu^{4+}, ^{12}C^{3+} and ^{4}He^{1+} ions were used with energies of 9.9 MeV, 8.3 MeV, 6.0 MeV and 0.5 MeV, respectively. The scattering angle from beam to the spectrometer was 42.5° as the sample tilt angle from the beam direction was varied from 80º to 88° with respective to the sample surface normal. In the analysis, elemental energies were calculated from the ToF-data and energy detector signal was only used for mass separation [18].

Results and Discussion

In TEM measurements it was found that Al$_2$O$_3$ and TiO$_2$ layers are well resolved at the 2–3 nm thickness level and that the nanolaminate surface remains flat also after several layers (Fig. 1). The surface smoothness was confirmed by atomic force microscope measurements which showed surface roughness (RMS) to be less than 0.2 nm for all the films in this study.

Prior to high resolution measurements, the samples were first measured with 9.9 MeV ^{35}Cl^{5+} beam in reflectance geometry, i.e. both angle of incidence and exit angle were 69º from the

sample normal. The results presented in Fig. 2 show that thinnest individual layers cannot be separated but the integrated elemental composition of the nanolaminates could be determined. In order to achieve better depth resolution, samples were tilted to an angle of 84º with respect to the sample normal. This evidently improves the depth resolution but has the drawback that the increased tilt enhances the detrimental effect of multiple and plural scattering [19] [20] and therefore worsened depth resolution deeper in the nanolaminate film. The effect of the plural scattering can be seen for example from the raw data ToF-E histogram in Fig. 3a as a persistent low energy tail for oxygen recoils. At this tilt angle, plural scattering can still be tolerated as seen from the depth profiles (Fig. 3b). However, if the tilt angle would further be increased, the top layers would be better resolved but the information from deeper in the sample would be smeared out.

From the measurements with 6 MeV $^{12}C^{3+}$ beam only events from the forward scattered carbon were used in the analysis, although also recoiled hydrogen, oxygen and aluminium could be identified in the ToF-E histogram (Fig. 4a). In this case the analysis using SimNRA [21] simulations were used to determine the layer separation and Ti, Al and O compositions. In the measurements with 500 keV incident $^{4}He^{1+}$ beam three to four 1 nm thick layers from the surface of the sample R5 could be separated if an extreme tilt angle of 88° was used. More reliable analysis could be made for the 2 nm nanolaminate sample R4 (see figure 4b) where up to 4×2 nm layers for both Al_2O_3 and TiO_2 could be clearly separated.

Measurements with the $^{63}Cu^{4+}$ incident beam did not anymore show uniform depth distributions for titanium, the heaviest element in the nanolaminate film. The measurements with 8.3 MeV $^{63}Cu^{4+}$ were considerable degraded by multiple and plural scattering especially in the case of Ti.

If higher beam energy would have been available, these effects would have been much reduced at cost of lower depth resolution.

From the measurements performed with different incident ions, the following observations were made. Firstly, analyzed nanolaminate compositions and thicknesses closely match the targeted values (see table 1) in the case of film thickness of 5 nm or higher. For the nanolaminate with layer thicknesses of 5 nm, following average concentrations were measured: O (59 ± 1.6) at.%, Al (18.5 ± 0.8) at.% and Ti (20.5 ± 0.7) at.%. In these concentrations the different number of Al_2O_3 and TiO_2 layers (see table 1) are taken into account. The nanolaminate films composed of thinner individual layers seem to have slightly different Al/Ti-ratio. Where thickest samples have Al/Ti-ratio close to 0.9, the R4 with 2 nm layers have Al/Ti-ratio more close to 0.8 and in the thinnest sample R5 the Al/Ti-ratio is closing to 0.7. This effect can also be seen from the Fig. 2 by comparing R3, R4 and R5 aluminium and titanium concentrations. This change in Al/Ti-ratio can either be due to enhanced growth rate of TiO_2, reduced growth rate or non-stoichiometric growth of Al_2O_3 during the first cycles or etching of Al_2O_3 due to TiO_2 pulses. In the high resolution (large sample tilt) measurements we could depth profile all 10 nm layers and separate also all 5 nm layers by means of 9.9 MeV $^{35}Cl^{5+}$ beam. For thinnest nanolaminate films only surface layers could be resolved with $^{35}Cl^{5+}$ beam. Forward scattered 6 MeV $^{12}C^{3+}$ beam satisfactorally resolved all the 10 and 5 nm thick layers, despite the kinematic broadening effect of Ti isotopes (Fig. 4a). The outer surface layers of the thinnest 1 nm sample R5 can also be identified with scattering 0.5 MeV He^{1+} beam but the Ti and Al peaks are fully overlapping due to the small difference in the kinematic factor of the scattering.

 In addition to the main film components Al, Ti and O, impurities could also be determined in the ToF-ERDA measurements with $^{35}Cl^{5+}$ and ^{63}Cu incident beams. From the analyses it was found

that most of the detected carbon comes from the surface impurities but also small, slightly varying carbon content was measured to be (0.16 ± 0.07) at.% in all nanolaminates films. Higher concentration of hydrogen is present throughout all the films and not only at the surface or at the nanolaminate-Si interface. The hydrogen impurity level in the film bulk was (1.5 ± 0.4) at.% in all the samples. The chlorine impurity was revealed by the heavier [63]Cu incident ion beam. Chlorine contamination originating from the $TiCl_4$ precursor gradually increases by a factor of 2 from thickest to thinnest sample and is at maximum 0.4 at.%. Elemental losses due to the ion bombardment were monitored and only significant loss was the one for the surface hydrogen.

Conclusions

We have performed the ion beam, TEM and AFM analysis for $Al_2O_3+TiO_2$ nanolaminates with different layer and film thicknesses. It could be concluded that film growth is uniform throughout the film stack and resulting laminates are smooth from the surface. Individual 10 nm and 5 nm layers could be distinguished through the whole nanolaminate film stack with high resolution ToF-ERDA measurements using 9.9 MeV [35]Cl[5+] beam and also by means of forward scattered 6 MeV [12]C[3+] ions. Use of 0.5 MeV [4]He[1+] ions is not favored because of fairly light element composition of the nanolaminate. Impurities of H, C and Cl could be measured down to 0.1 at.% level.

References

[1] Mikko Ritala, Markku Leskelä, Handbook of Thin Films, Elsevier, Los Angeles, 2002, pp. 103-159.

[2] T. Suntola, J. Antson, A. Pakkala, S. Lindfors, SID 80 Digest (1980) 108.

[3] M. Putkonen, T. Sajavaara, P. Rahkila, L. Xu, S. Cheng, L. Niinistö, H.J. Whitlow, Thin Solid Films, 517 (2009) 5819.

[4] A.R. Sagari, P. Rahkila, M. Väisänen, R. Lehto, T. Sajavaara, S. Gorelick, M. Laitinen, M. Putkonen, S. Sangyuenyongpipat, J. Timonen, S. Cheng, H.J. Whitlow, Nucl. Instr. and Meth. B, 266 (2008) 2515.

[5] M. Law, L.E. Greene, A. Radenovic, T. Kuykendall, J. Liphardt, P. Yang, J. Phys. Chem. B, 110 (2006) 22652.

[6] J. Robertson, Rep. Prog. Phys. 69 (2006) 327.

[7] R.L. Puurunen, J. Saarilahti, H. Kattelus, ECT Transactions 11 (2007) 3.

[8] J.W. Elam, Z.A. Sechrist, S.M. George, Thin Solid Films, 414 (2002) 43–55.

[9] M. Heikkilä, E. Puukilainen, M. Ritala, M. Leskelä, J. Photochem. Photobiol. A. 204 (2009) 200.

[10] K. Kukli, J. Ihanus, M. Ritala, M. Leskelä, Appl. Phys. Lett. 68 (1996) 3737.

[11] M. Ritala, M. Leskelä, L. Niinistö, T. Prohaska, G. Friedbacher, M. Grasserbauer, Thin Solid Films 249 (1994) 155.

[12] M.B. Daia, P. Aubert, S. Labdi, C. Sant, F.A. Sadi, P. Houdy, J.L. Bozet, J. Appl. Phys. 87 (2000) 7753.

[13] Y. S. Kim, S. J. Yun, J. Crystal Growth, 274 (2005) 585.

[14] P.C. Rowlette, C.A. Wolden, Thin Solid Films, 518 (2010) 3337.

[15] J.K. Kim, Y.S. Kim, G.D. Kim, H.W. Choi, H.J. Woo, S.Y. Cho, C.N. Whang, Nucl.

Instr. and Meth. B 140 (1998) 380.

[16] S. Giangrandi, T. Sajavaara, B. Brijs, K. Arstila, A. Vantomme, W. Vandervorst, Nucl. Instr. and Meth. B, 266 (2008) 5144.

[17] F. Busch, W. Pfeffer, B. Kohlmeyer, D. Schüll, F. Pühlhoffer, Nucl. Instr. and Meth. 171 (1980) 71.

[18] M. Hult, H.J. Whitlow and M. Östling, Appl. Phys. Lett. 60 (1992) 219.

[19] K. Arstila, T. Sajavaara, J. Keinonen, Nucl. Instr. and Meth. B, 174 (2001) 163.

[20] S. Giangrandi, K. Arstila, B. Brijs, T. Sajavaara, A. Vantomme, W. Vandervorst, Nucl. Instr. and Meth. B, 267 (2009) 1936.

[21] M. Mayer, SIMNRA User's Guide, Report IPP 9/113, Max-Planck-Institut für Plasmaphysik, Garching, Germany, 1997.

Tables

Table 1. ALD nanolaminates prepared on 150 mm Si wafers. In the deposition $Al(CH_3)_3$ and H_2O precursors were used for Al_2O_3 and $TiCl_4$ and H_2O precursors for TiO_2. The growth temperature was 200 ºC.

| Sample | Number of ALD cycles and nominal sample thicknesses (**nm in parenthesis**). Al_2O_3 is always the outermost layer. | | | |
	Al_2O_3, cycles per layer	TiO_2, cycles per layer	Number of Al_2O_3 + TiO_2, layers	Tot. **nm**
R1	207 (**20**)	493 (**20**)	*2 + 1*	(**60**)
R2	104 (**10**)	257 (**10**)	*3 + 2*	(**50**)
R3	52 (**5**)	123 (**5**)	*5 + 4*	(**45**)
R4	21 (**2**)	49 (**2**)	*11 +10*	(**42**)
R5	10 (**1**)	25 (**1**)	*21 + 20*	(**41**)

List of figure captions

Figure 1. TEM micrograph of 45 nm thick nanolaminate, with individual Al_2O_3 and TiO_2 layer thicknesses of 2 nm and 3 nm, respectively.

Figure 2. Samples with 20, 10, 5, 2 and 1 nm layer thicknesses measured with 9.9 MeV $^{35}Cl^{5+}$ incident ions. The angle of incidence was 69° with respect to the sample normal.

Figure 3. Sample R2 (10 nm layer thickness) measured with 9.9 MeV $^{35}Cl^{5+}$ at 84° incident angle. In a) a histogram of the raw spectra is shown and in b) the corresponding elemental depth profiles. Scattered ^{35}Cl beam was used for depth profiling Ti. Total concentration for each depth is scaled to 100 at.%.

Figure 4. a) Sample R3 (5 nm layers) measured with 6 MeV $^{12}C^{3+}$ at 84° incident angle. Data analyzed by SimNRA [21] simulation which closely matches in all 9 x 5 nm layers. b) Sample R4 (2 nm layers) measured with 500 keV $^{4}He^{1+}$ at 87° incident angle. Only first 7-9 layers can be separated in the SimNRA fit. Inserts in the figures show the raw ToF-E spectra.

Figure 1

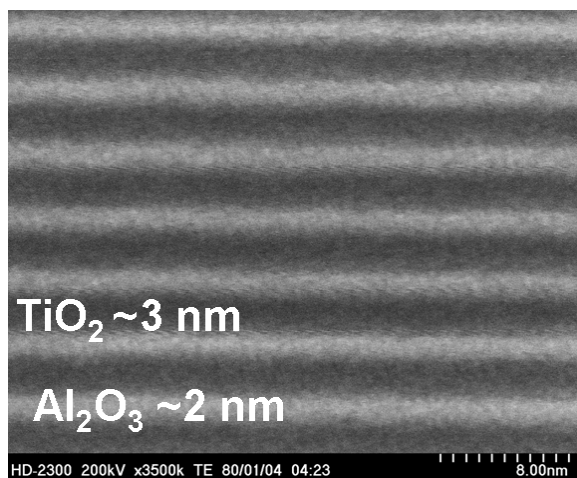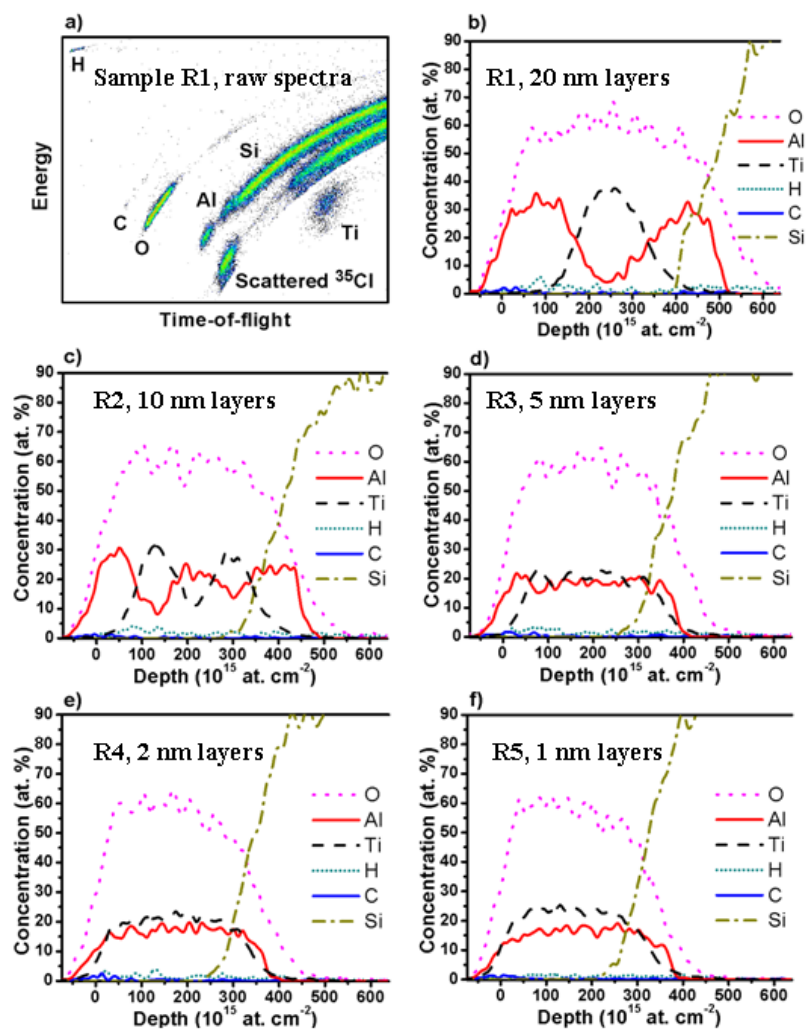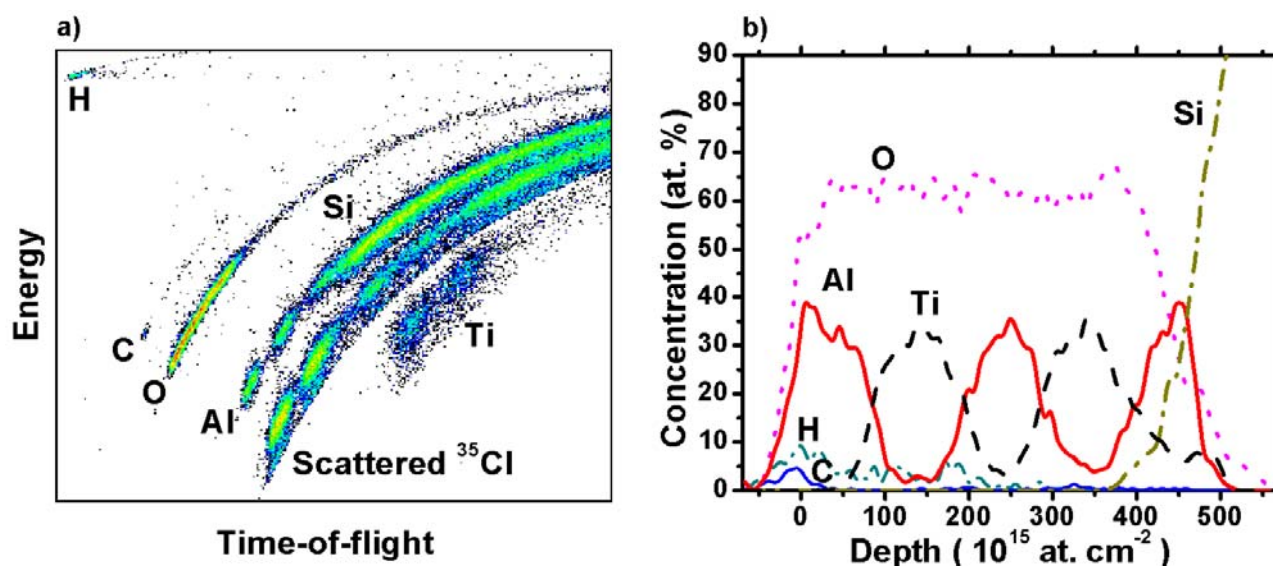TiO$_2$ ~3 nm

Al$_2$O$_3$ ~2 nm

HD-2300 200kV x3500k TE 80/01/04 04:23   8.00nm

Figure 2

Figure 3

Figure 4